THE JOURNAL OF BIOLOGICAL CHEMISTRY VOL. 281, NO. 38, pp. 28318–28325, September 22, 2006
© 2006 by The American Society for Biochemistry and Molecular Biology, Inc. Printed in the U.S.A.

CprK Crystal Structures Reveal Mechanism for Transcriptional Control of Halorespiration*

Received for publication, March 21, 2006, and in revised form, June 23, 2006 Published, JBC Papers in Press, June 27, 2006, DOI 10.1074/jbc.M602654200

M. Gordon Joyce[‡], Colin Levy[‡], Krisztina Gábor[§], Stelian M. Pop[¶], Benjamin D. Biehl[¶], Tzanko I. Doukov[‖], Jodi M. Ryter[**], Hortense Mazon[‡‡], Hauke Smidt[§], Robert H. H. van den Heuvel[‡‡], Stephen W. Ragsdale[¶], John van der Oost[§], and David Leys[‡1]

From the [‡]Manchester Interdisciplinary Biocentre, P. O. Box 88, Manchester, M60 1QD, United Kingdom, the [§]Laboratory of Microbiology, Wageningen University, Hesselink van Suchtelenweg 4, 6703 CT Wageningen, The Netherlands, the [¶]Department of Biochemistry, Beadle Center, University of Nebraska, Lincoln, Nebraska 68588-0664, the [‖]Stanford Synchrotron Radiation Laboratory, Menlo Park, California 94025, the [**]Department of Chemistry, Nebraska Wesleyan University, Lincoln, Nebraska 68504-2794, and the [‡‡]Department of Biomolecular Mass Spectrometry, Bijvoet Center for Biomolecular Research and Utrecht Institute for Pharmaceutical Sciences, Utrecht University, Sorbonnelaan 16, 3584-CA Utrecht, The Netherlands

Halorespiration is a bacterial respiratory process in which haloorganic compounds act as terminal electron acceptors. This process is controlled at transcriptional level by CprK, a member of the ubiquitous CRP-FNR family. Here we present the crystal structures of oxidized CprK in presence of the ligand *ortho*-chlorophenolacetic acid and of reduced CprK in absence of this ligand. These structures reveal that highly specific binding of chlorinated, rather than the corresponding non-chlorinated, phenolic compounds in the NH_2-terminal β-barrels causes reorientation of these domains with respect to the central α-helix at the dimer interface. Unexpectedly, the COOH-terminal DNA-binding domains dimerize in the non-DNA binding state. We postulate the ligand-induced conformational change allows formation of interdomain contacts that disrupt the DNA domain dimer interface and leads to repositioning of the helix-turn-helix motifs. These structures provide a structural framework for further studies on transcriptional control by CRP-FNR homologs in general and of halorespiration regulation by CprK in particular.

Past and present industrial and agricultural activities have led to the ever increasing presence of haloorganic compounds such as chlorophenols and chlorinated ethenes in the environment (1). Due to both toxicity and recalcitrant nature, increasing amounts of these xenobiotics threaten the integrity of the environment and human health (2). In recent years, it has emerged that several haloorganic compounds are also naturally produced (3) and that several species of strictly anaerobic bacteria are able to conserve energy via the reductive dehalogenation of these compounds by respiratory metabolism (4, 5). In view of their favorable degrading capacities, *e.g.* high dehalogenation rate and low residual concentration of the contaminant, it has been anticipated that halorespiring microorganisms should be of utmost significance for efficient biological remediation of halogenated hydrocarbons in anoxic environments (6, 7). The versatile, strictly anaerobic Gram-positive bacterium *Desulfitobacterium dehalogenans* and the closely related *Desulfitobacterium hafniense* have the capacity of degrading *ortho*-chlorophenol. Both have been used as model organisms in halorespiration studies, representing one of the most significant groups of halorespiring isolates (8). In these organisms, proteins involved in halorespiration are encoded by the *cpr* (chlorophenol reductive dehalogenase) operon, of which multiple copies are present within the genome. This potentially allows for reductive dehalogenation of a wide range of haloorganic compounds by the use of a series of paralogous enzymes (9).

The *cpr* operon is transcriptionally regulated by CprK, a member of the CRP-FNR family of regulators that is ubiquitous in bacteria (10). Recent *in vivo* and *in vitro* studies reveal that CprK binds 3-chloro-4-hydroxyphenylacetate (CHPA)[2] with micromolar affinity promoting a tight interaction with a specific DNA sequence in the promoter region of the *cpr*-encoded genes, called the "dehalobox" (11, 12). CHPA-like compounds that lack either the chloride or the hydroxyl group fail to induce DNA binding, even at millimolar concentrations. The *cpr* gene cluster appears to be subject to a second layer of transcriptional control; under aerobic conditions, oxidation of CprK leads to disulfide bond formation, which prevents DNA binding (11).

Regulators of the CRP-FNR family respond to a broad spectrum of intracellular and exogenous signals (13). To accomplish their roles, these regulatory proteins have intrinsic sensory modules that either bind allosteric effector molecules or chemically modulate prosthetic groups, after which a signal is trans-

* This work was funded in part by the Biotechnology and Biological Sciences Research Council, United Kingdom. Work on the *D. dehalogenans* CprK was supported in part by National Science Foundation Grant MCB9974836 (to S. W. R.). The costs of publication of this article were defrayed in part by the payment of page charges. This article must therefore be hereby marked "*advertisement*" in accordance with 18 U.S.C. Section 1734 solely to indicate this fact.

The atomic coordinates and structure factors (code 2H6B and 2H6C) have been deposited in the Protein Data Bank, Research Collaboratory for Structural Bioinformatics, Rutgers University, New Brunswick, NJ (http://www.rcsb.org/).

[1] A Royal Society University Research Fellow and an European Molecular Biology Organization Young Investigator. To whom correspondence should be addressed. Tel.: 44-161-306-51-50; Fax: 44-161-275-55-86; E-mail: david.leys@manchester.ac.uk.

[2] The abbreviations used are: CHPA, 3-chloro-4-hydroxyphenylacetate; MES, 4-morpholineethanesulfonic acid; r.m.s.d., root mean square deviation; ESI, electrospray ionization; MS, mass spectrometry; dsDNA, double-stranded DNA; HPA, *ortho*-hydroxyphenolacetic acid.

Downloaded from www.jbc.org at UKB - Universiteitbibliotheek Utrecht on November 16, 2006

mitted to a DNA-binding domain. For example, the paradigmatic *Escherichia coli* cAMP receptor protein (CRP) undergoes a conformational change upon binding cAMP that triggers binding to the promoter region of target genes (14). To date, crystal structures of distinct CRP states provide atomic insights into cAMP-, DNA-, and RNA-polymerase binding (15–17). However, a detailed structure for the ligand-free, non-DNA binding state of CRP is lacking. The structural data available for other CRP-FNR family members are limited to the crystal structures of CooA from *Rhodospirillum rubrum* (18) and the pathogenicity factor PrfA from *Listeria* spp (19), both ligand-free structures. Due to the absence of a family member with both ligand-bound and -free states available, the allosteric mechanism by which effector binding induces a conformational transition to an "active," DNA binding state is poorly understood, and several models have been put forward to explain how the sensory module can transmit the signal to the distant DNA-binding domain (14, 15, 20, 21).

Here we report the 2.2-Å crystal structure of the oxidized *D. hafniense* CprK in the presence of CHPA and the 2.9-Å crystal structure of the highly related *D. dehalogenans* CprK (both proteins are 232 amino acids long and 89% identical) in the ligand-free, reduced state. Comparison of both structures allows identification of the allosteric changes induced by ligand binding.

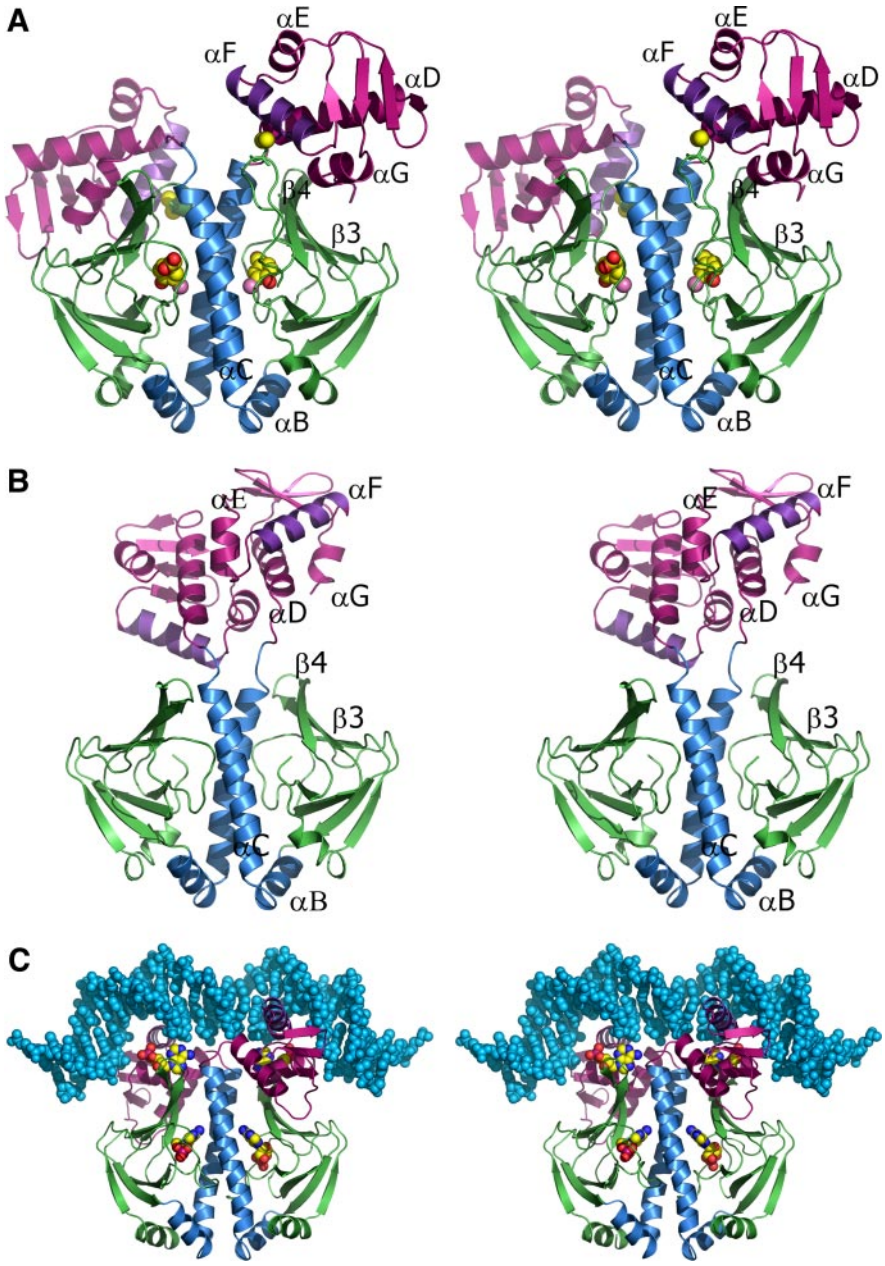

FIGURE 1. **Crystal structures of CprK and comparison with cAMP-CRP-DNA complex.** *A*, stereo view of the crystal structure of the oxidized ligand-bound CprK from *D. hafniense* in cartoon representation. The NH_2-terminal β-barrels are colored *green*, the α-helices B and C are colored *blue*, the COOH-terminal DNA-binding domains are colored *pink* with the exception of the DNA-binding helix of the helix-turn-helix motif, which is in *purple*. The bound CHPA and the intermolecular disulfide bond between Cys-11 and Cys-200 are represented in atom-colored spheres. Distinct secondary elements are labeled for domains to the *right side* of the dimer. *B*, stereo view of the crystal structure of the reduced ligand-free CprK from *D. dehalogenans* in schematic representation. Color coding is according to *A*. *C*, the crystal structure of *E. coli* CRP in complex with DNA and cAMP (Protein Data Bank code 1CRG) in schematic representation. Color coding is according to *A* with representation of bound cAMP molecules in atom-colored spheres and DNA in *blue spheres*.

MATERIALS AND METHODS

Crystallization and Structure Elucidation of D. hafniense Cpr—Cprk was prepared as described previously (12), using the pWUR89 expression vector. Crystals of the oxidized CprK-CHPA complex were grown in 100 mM Tris, pH 7.5, 1.8 M ammonium sulfate at 4 °C. Heavy atom derivatization of the crystals was carried out by soaking crystals in mother liquor containing 10 mM potassium tetrachloroplatinate(II) and 10 mM mercury(II) acetate. Data were collected on single crystals at Deutsches Elektron-Synchrotron (DESY), Hamburg, Germany, beamline BW7A. All data were processed and scaled using DENZO and SCALEPACK (22), and crystals belong to the I222 space group (a = 104.4 Å, b = 112.2 Å, c = 119.5 Å). The position of heavy atom sites for isomorphous derivatives was found using difference Patterson functions and verified using (cross) difference Fourier analysis. Coordinates and real and anomalous occupancies were refined for all heavy atom positions and final MIRAS phases calculated using MLPHARE (23). Density modification and non-crystallographic symmetry averaging were carried out using DM (24). Model building was carried out using TURBO-FRODO (25), and maximum like-

Downloaded from www.jbc.org at UKB - Universiteitsbibliotheek Utrecht on November 16, 2006

lihood refinement was carried out using REFMAC5 (26). Final coordinates and structure factors have been deposited with the Protein Data Bank (codes 2H6B and RCSB037983, respectively).

Crystallization and Structure Elucidation of D. dehalogenans CprK—CprK was expressed and purified as described previously (11). CprK (7–8 mg/ml) was crystallized in a solution containing 100 mM MES pH 6.5, 115 mM $MgCl_2$, 8% polyethylene glycol-3350, and 10 mM dithiothreitol. Data were collected from a single flash-cooled crystal at beamline 11-1 at Stanford Synchrotron Radiation Laboratory. All data were processed and scaled using Crystal Clear (27), and crystals belong the the $P2_1$ space group (a = 72.7 Å, b = 50.0 Å, c = 76.4 Å, β = 105.5°). Molecular replacement using the individual domains of the *D. hafniense* CprK was carried out using Phaser (28). Model building was carried out using TURBO-FRODO (25) and COOT (29). Maximum likelihood and translation-libration-screw refinement were carried out using REFMAC5 (26, 30). Final coordinates and structure factors have been deposited with the Protein Data Bank (codes 2H6C and RCSB037984, respectively).

Trp Fluorescence Quenching—Fluorescence experiments were carried out using a Cary Eclipse fluorescence spectrophotometer with constant temperature at 25 °C maintained using a Cary single cell peltier regulator. Samples were measured using a Hellma precision quartz cuvette with a 10-mm light path. Excitation was carried out at 295 nm with a 5 nm wavepath and emission fluorescence measured at 370 nm with a 10 nm wavepath. CHPA was added to a 1-ml solution of 10 μM wild-type or mutant CprK in 50 mM potassium phosphate buffer, pH 7.2. Quenching observed was corrected for the inner filter effect by titration of CHPA *versus* tryptophan. To determine the binding constant for *ortho*-hydroxyphenolacetic acid (HPA), titrations *versus* CHPA were carried out in the presence of 1–10 mM HPA.

Native Macromolecular Mass Spectrometry—4 μM CprK dimer was used for mass spectrometry studies in the presence of 10 mM dithiothreitol. For DNA binding measurements, 4 μM CprK was incubated with 400 μM CHPA and 5 μM dsDNA for 30 min at room temperature. Native macromolecular mass spectrometry measurements were performed in positive ion mode using an electrospray ionization time-of-flight instrument (LC-T; Micromass, Manchester, UK) equipped with a Z-spray nano-electrospray ionization source. To produce intact ions *in vacuo* from large complexes in solution the ions were cooled by increasing the pressure in the first vacuum stages of the mass spectrometer (31, 32). Source pressure conditions and electrospray voltages were optimized for transmission of the macromolecular protein complexes (31). The needle and sample cone voltage were 1,400 and 140 V, respectively. The pressure in the interface region was adjusted to 8 millibars. The spectra were mass calibrated by using a solution of 10 mg/ml cesium iodide in isopropanol: water 50:50. Deconvoluted spectra were generated by using the transform tool of the MassLynx software.

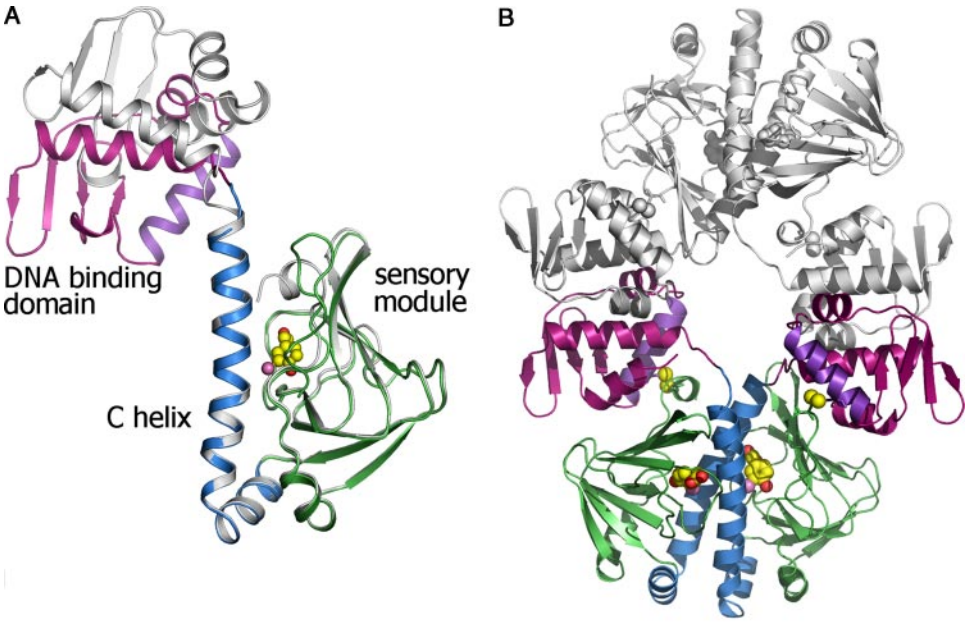

FIGURE 2. **Oligomeric structure of oxidized CprK.** *A*, overlap of both monomers within the oxidized CprK dimer observed in the asymmetric unit. One monomer is colored *gray*, while the other is colored as described for Fig. 1. *B*, schematic representation of the putative tetrameric CprK molecule obtained by applying 2-fold crystal symmetry; one CprK dimer is colored *gray*, while the other is colored as described for Fig. 1.

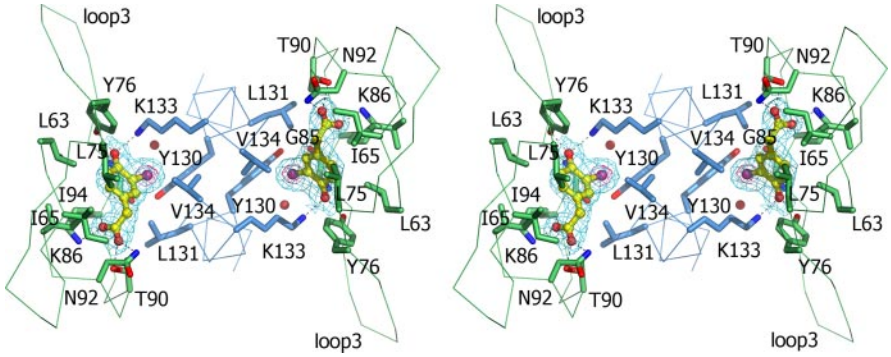

FIGURE 3. ***D. hafniense* CprK CHPA-binding site.** Stereo representation of the binding site for CHPA with key residues depicted in sticks in addition to the Cα trace for residues 63–94 (part of the β-barrel) and 129–135 (part of the C helix). Color coding is the same as described for Fig. 1. Hydrogen bonds between binding site residues and CHPA are indicated by *black dashed lines*. The SigmaA weighted F_oF_c omit map is superimposed on the bound CHPA molecules contoured at 3σ (in *blue*) and 6σ (in *magenta*).

RESULTS AND DISCUSSION

Crystal Structure of Oxidized, Ligand-bound D. hafniense CprK—The crystal structure of oxidized *D. hafniense* CprK in complex with CHPA was determined to 2.2 Å

Downloaded from www.jbc.org at UKB - Universiteitsbibliotheek Utrecht on November 16, 2006

using MIRAS and non-crystallographic symmetry averaging techniques (Fig. 1*A*). The asymmetric unit contains a single CprK dimer with each monomer folded in two distinct domains connected by a long α-helix. The r.m.s.d. in the Cα position between both monomers in the asymmetric unit is 0.455 Å for the DNA-binding domain and 0.256 Å for the sensory module. A search of the protein structure data base reveals that CprK is most similar to CRP (Protein Data Bank code 2CGP; Fig. 1*C*) (sensory module: Z score of 13.9 and r.m.s.d. of 3.0 Å for 124 Cα atoms; DNA-binding domain: Z score of 9.3 and r.m.s.d. of 1.9 Å for 68 Cα atoms). The relative position of the sensory modules within the CprK dimer is similar to CRP, the dimer interface predominantly made by the C α-helices. However, in contrast to CRP and other crystal structures of related regulators, CprK is a-domain swapped dimer, with the COOH-terminal DNA-binding domain of one monomer interacting with the NH_2-terminal effector-binding domain of the other. While a non-crystallographic 2-fold axis relates both sensory modules, the relative position of both DNA-binding domains is drastically different, resulting in a distinctly asymmetric CprK dimer (Fig. 2*A*). Within the dimer, two intersubunit disulfide bonds are present between Cys-11 from the sensory module and Cys-200 located in the DNA-binding helix F. For both DNA-binding domains, contacts with β-strands 3 and 4 of the sensory module are mainly made by residues of the COOH-terminal helix G (not present in CRP), leading to a surface area buried of, respectively, ~70 $Å^2$ and ~220 $Å^2$ for the individual contacts. In contrast, in the CRP-DNA complex (Fig. 1*C*), contacts between β-strands 4 and 5 and the DNA-binding domain occur via residues provided by helices D and E. Thus, whereas in CRP both DNA-binding helices are positioned roughly perpendicular to the central α-helical pair along the same face of the molecule, the CprK DNA-binding helices are near parallel to the C α-helices. This conformation is not compatible with tight binding to the dehalobox DNA. Reorientation of both domains to a position similar to that observed in CRP-DNA complexes requires breaking the disulfide bond between Cys-11 and Cys-200 and reorientation of the NH_2-terminal polypeptide stretch preceding Pro-16. In CRP, residues from helices D and E are involved in interdomain contacts; surprisingly, the corresponding residues for both CprK DNA domains are in close contact with the same residues from a symmetry related dimer (Fig. 2*B*). The interface formed between two CprK dimers involves the close association of four DNA-binding domains: a 870-$Å^2$ surface that is mainly hydrophobic, containing four salt bridges in addition to several hydrogen bonds. The interface has a surface complementarity 0.68 (33) suggesting it is a physiologically relevant interaction in the non-DNA binding state.

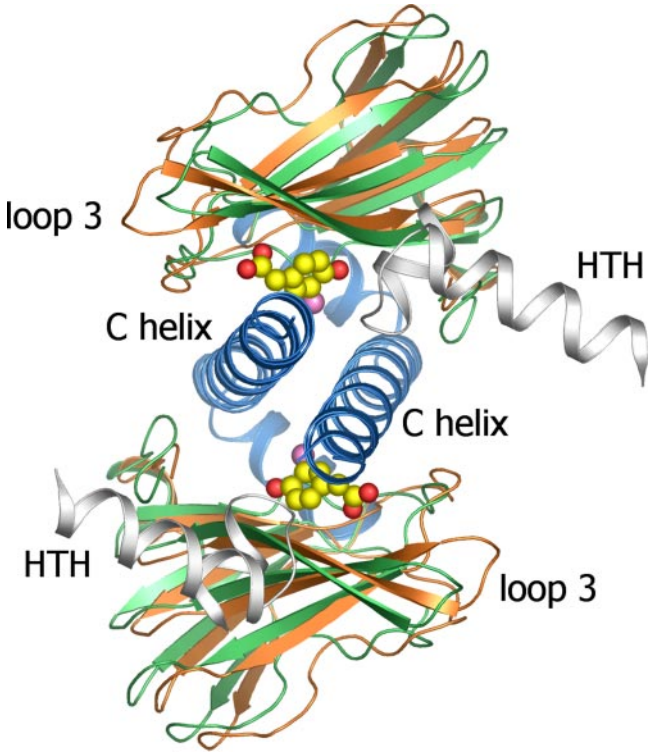

FIGURE 4. **Overlay of the NH_2-terminal domains of both CprK structures.** An overlay is shown that was created by superimposition of the B and C α-helices of both ligand-free CprK and the CHPA-bound CprK structures with central helices colored *blue* for both structures, while the NH_2-terminal β-barrel (residues 20–108 for both structures) is colored *green* for the CHPA-CprK complex and *orange* for the ligand free CprK. Bound CHPA molecules in the CHPA-CprK structure are represented in atom-colored spheres. To illustrate the motion of the NH_2-terminal β-barrel with respect to the putative position of the HTH motifs in the DNA binding state (by analogy to CRP), the putative HTH motifs are represented in *gray*.

CHPA Binding by CprK—Clear electron density is observed for a tightly bound CHPA molecule in the sensory modules of both monomers in a position similar to the binding site of cAMP in CRP (Fig. 3). CprK makes six direct hydrogen bonds to CHPA and two salt bridge contacts, one between Lys-86 and the acetate group of the effector and another between the CHPA phenol hydroxyl group (assuming this is deprotonated) and the conserved residue Lys-133. The phenol hydroxyl group forms hydrogen bonding contacts with Tyr-76 (2.3 Å), Lys-133 (2.7 Å), and the backbone nitrogen of Gly-85 (3.0 Å) of one monomer. The chloride atom is positioned in van der Waals contact with residues of the

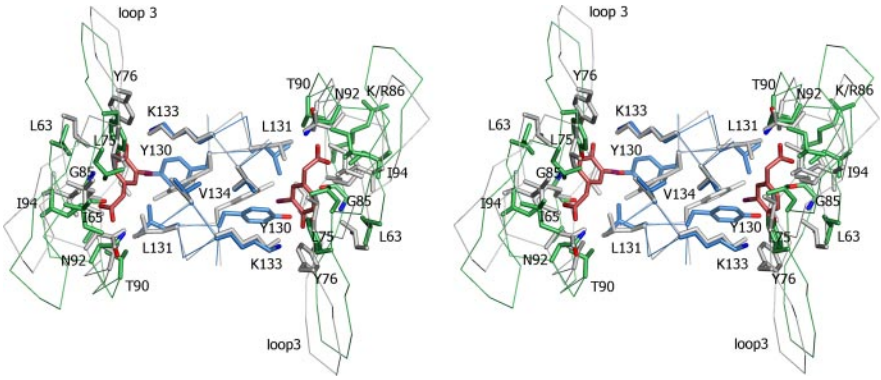

FIGURE 5. **Overlay of the CHPA-binding sites of both CprK structures.** Using a similar superimposition as Fig. 4, the key binding site residues for both CprK structures are represented as described for Fig. 3. The CHPA-CprK structure is colored with *gray* carbon atoms (CHPA with *purple* carbon atoms), while the ligand-free CprK structure is represented with carbon atoms colored as described for to Fig. 1.

Downloaded from www.jbc.org at UKB - Universiteitsbibliotheek Utrecht on November 16, 2006

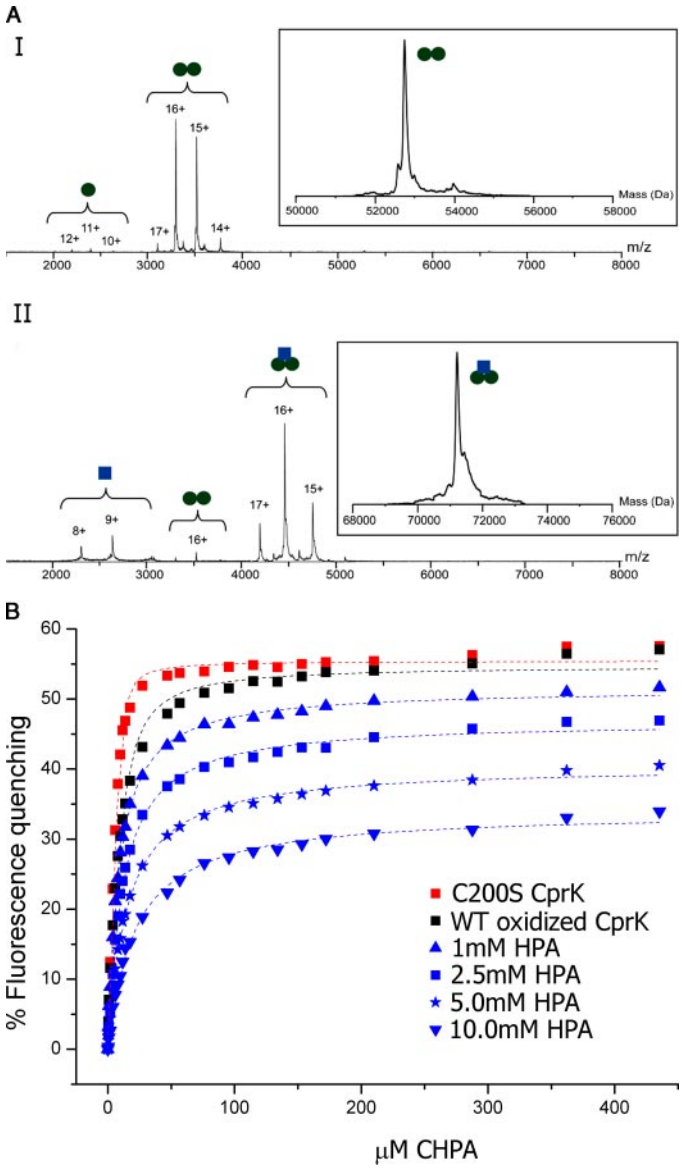

FIGURE 6. **Solution data on *D. hafniense* CprK.** *A*, native ESI-MS data. ESI-MS spectra of *D. hafniense* CprK sprayed from an aqueous 100 mM ammonium acetate solution, pH 8, at a dimer concentration 4 μM in the presence of 10 mM dithiothreitol (*I*) and in the presence of 5 μM dsDNA and 400 μM CHPA (*II*). The charges of the different ion series are indicated. The *green circle* and *blue square* indicate monomeric CprK and dehalobox DNA, respectively. The *insets* represent the deconvoluted mass spectra of dimeric CprK (*I*) and the complex between CprK and dsDNA (*II*). *B*, Trp fluorescence quenching by CHPA titration. Tryptophan fluorescence quenching obtained by titration of C200S *D. hafniense* CprK and oxidized wild-type (*WT*) *D. hafniense* CprK with CHPA, in the presence or absence of HPA. Data were fitted to a single exponential quadratic function.

central α-helix of the opposite monomer. The binding pocket for the chloride atom is made up of hydrophobic residues Tyr-130 (3.7 Å), Leu-131 (3.8 Å), and Val-134 (3.9 Å) in addition to a buried water molecule (3.9 Å), several main chain atoms of Gly-85 (3.7 Å) and the Lys-133 amino-terminal group (3.6 Å). The CHPA acetic acid group is hydrogen bonded to Lys-86 (2.7 Å), Thr-90 (2.6 Å), and Asn-92 (2.8 Å), while the aromatic moiety is sandwiched between several hydrophobic residues in the β-barrel.

Crystal Structure of Reduced, Ligand-free D. dehalogenans CprK—The crystal structure of the reduced *D. dehalogenans* CprK was solved to 2.9 Å by molecular replacement using the individual *D. hafniense* CprK domains as search models. The asymmetric unit contains a single CprK dimer with the sensory modules and central α-helix coiled coil in highly similar orientations as observed for oxidized CprK (Fig. 1, *A and B*). The r.m.s.d. in Cα position between both monomers in the asymmetric unit is 0.251 Å for the DNA-binding domain and 0.319 Å for the sensory module. Close comparison of both the ligand-free and ligand-bound sensory modules reveals no significant change in the relative position of helices B and C, which provide the majority of the CprK dimer interface (r.m.s.d. 0.3 Å for 46 Cα atoms). In contrast, the positions of both NH_2-terminal β-barrels have shifted with respect to the B and C helices in the ligand-free structure (Fig. 4). The motion relating the position of the NH_2-terminal β-barrel in both crystal structures constitutes a rigid body hinge movement around residue Ser 108 immediately preceding helix B. This leads to a maximum shift in position of ~3.8 Å for β-strands 4 and 5. Due to the relatively small shift in position and the flexibility of some side chains, many of the direct contacts between the β-barrel and the central C helix are conserved between both conformations. The CHPA-binding site is empty (water molecules cannot be reliably observed at this resolution) and is part of a tunnel extending across the molecule and providing solvent access. While the residues involved in binding CHPA are completely conserved between both *D. hafniense* and *D. dehalogenans* CprK (except for the conservative replacement of Lys/Arg 86), they occupy different conformations in both crystal structures (Fig. 5). A notable exception being residue Lys 133 which does not show a ligation dependent conformational shift. The 3.7 Å shift in the Cα position of Gly 85 is one of the largest differences observed when comparing both structures.

TABLE 1
Observed K_d values for CHPA and HPA binding to *D. hafniense* CprK

Protein sample and ligand	K_d
	μM
Oxidized CprK + CHPA	4.1 ± 0.4
C200S CprK + CHPA	0.83 ± 0.11
Oxidized Y76F CprK + CHPA	14.39 ± 0.79
Y76F CprK + DTT + CHPA	10.24 ± 0.49
CprK + HPA	6206 ± 423

In contrast to the relatively minor changes observed in the sensory modules, the short linker regions connecting the C α-helix with the DNA-binding domain are projecting outward from the central coiled coil, positioning the DNA-binding domains at a distance from the sensory modules rather than the close contacts observed in the oxidized CprK structure. Both DNA-binding domains form a close association that buries hydrophobic residues from helices D and E and is identical to the dimerization observed between oxidized CprK dimers (Fig. 2*B*), providing further evidence for the physiological relevance of this interaction.

Native ESI-MS Reveals a Single CprK Dimer That Binds dsDNA in Presence of CHPA—The ESI-MS spectrum of *D. hafniense* CprK under reducing conditions (Fig. 6*A*) revealed that CprK is mainly dimeric with a measured mass of 52,739.4 ± 3.7 Da (calculated mass 52,736 Da). Fig. 6 shows the ESI-MS spectrum of CprK incubated with a 30-bp DNA frag-

Downloaded from www.jbc.org at UKB - Universiteitbibliotheek Utrecht on November 16, 2006

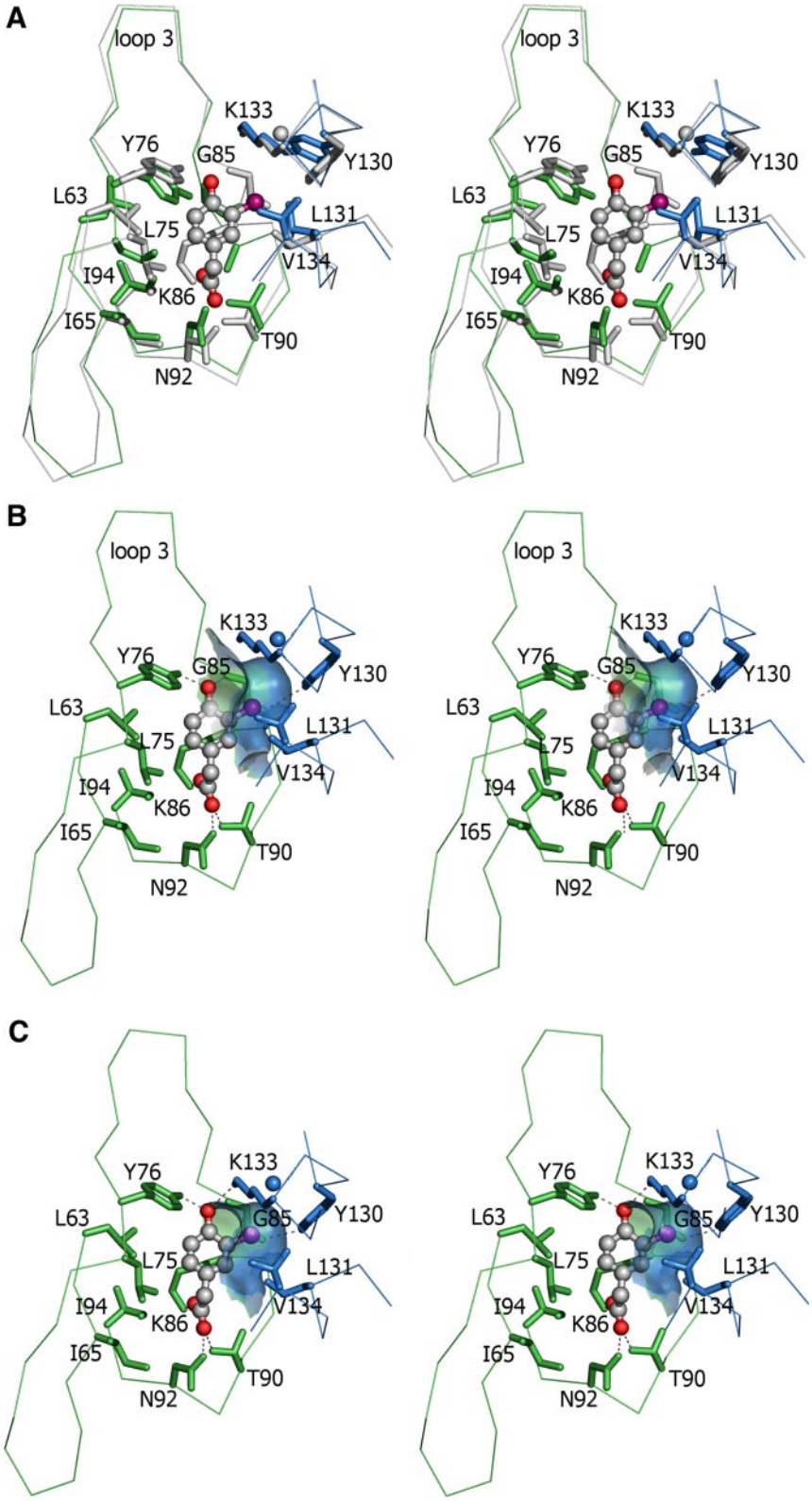

FIGURE 7. **Binding of *ortho*-chlorophenolic compounds causes structural rearrangement.** *A*, overlay of a single CHPA-binding site of the ligand-free CprK (color coding same as described for Fig. 1) with a hybrid CprK structure (in *gray*; see "Results and Discussion"). This clearly illustrates the induced fit in both the NH_2-terminal β-barrel and the C helix residues upon binding of CHPA. *B*, similar view to *A*, but only the hybrid structure is displayed, colored-coded as described for Fig. 1. The hydrophobic pocket created by the C helix residues is depicted as a transparent surface. H-bonds between CHPA and CprK are depicted in *dashed lines*. No direct interaction can be made between CHPA and Lys-133, while the CHPA chloride atom is not ideally placed in the binding pocket. *C*, similar view to *B* but for the CHPA-CprK crystal structure. The reorientation of the β-barrel has allowed for an additional interaction between CHPA and Lys-133 while positioning the CHPA chloride atom in the center of the hydrophobic cavity.

ment containing the dehalobox recognition site, and CHPA under reducing conditions. The spectrum clearly shows that dimeric CprK interacts specifically with one molecule of dsDNA (measured mass 71,165.0 ± 2.7) with very low amounts of free dsDNA and CprK present. The observed mass increase of the analyzed complex as compared with the calculated mass (71,143 Da) is likely due to water or buffer molecules still present in the protein-DNA complex. In the absence of CHPA, the level of CprK-DNA complex was very low. These results show that active CprK is a dimer that binds dehalobox DNA in equimolar amounts when CHPA is present.

Trp Fluorescence Quenching Indicates High Specificity for CHPA—Trp fluorescence quenching experiments demonstrate up to 55% quenching upon titration of oxidized *D. hafniense* CprK with CHPA, leading to an apparent K_d of 4.1 ± 0.4 μM for CHPA. This binding becomes slightly tighter (to an apparent K_d of 0.83 ± 0.11 μM) when using a C200S mutant (12) that is unable to form the disulfide bond (Fig. 6*B* and Table 1). A single Trp is situated at the bottom of the β-barrel, which is not in close contact with the CHPA-binding site. It is therefore most likely that binding of CHPA triggers a conformational change that results in the fluorescence quenching. Titration with HPA, which only differs from CHPA in lacking the chloride substituent, does not result in significant quenching even at millimolar concentrations. Binding of HPA to CprK can indirectly be observed through inhibition of CHPA-induced Trp fluorescence quenching, leading to an observed K_d for HPA of 6.2 ± 0.4 mM. Thus, despite the relatively small difference in structure, CprK has a remarkable preference for the chlorinated compound, in terms of both affinity (>1000-fold higher for CHPA over HPA) and functionality (HPA binding does not induce any measurable increase in DNA binding). Thus, the

Downloaded from www.jbc.org at UKB - Universiteitsbibliotheek Utrecht on November 16, 2006

TABLE 2
Crystallographic data collection and refinement parameters

	CprK *D. hafniense* (2H6B)	Potassium tetrachloroplatinate soak	Mercury acetate soak	CprK *D. dehalogenans* (2H6C)
Soak time/Concentration		10 min/10 mM	10 min/10 mM	
Space group	I 222	I 222	I 222	$P2_1$, $\beta = 105.5°$
Cell dimensions				
a (Å)	104.4	104.9	105.2	72.7
b (Å)	112.1	113.0	112.3	50.0
c (Å)	119.4	119.6	117.8	76.4
X-ray source[a]	DESY BW7A	DESY BW7A	DESY BW7A	11.1 SSRL
Resolution (Å)	50-2.2 (2.25-2.2)	50-2.5 (2.55-2.5)	50-3.1 (3.2-3.1)	50-2.9 (2.97-2.90)
No. of observations				
Total	766,373	313,230	423,430	54,952
Unique	35,512	24,333	12,468	16,387
Completeness (%)	99.2 (100)	97.6 (98.6)	95.8 (99.8)	99.0 (99.8)
$I/\sigma I$	16.6 (2.5)	17.08 (2.906)	8.97 (2.31)	10.6 (3.6)
R_{merge}	0.102 (0.573)	0.078 (0.427)	0.147 (0.415)	0.056 (0.257)
Model	Residues 3–250 for chain A, 9–243 for chain B, residues 233–250 are part of the COOH-terminal His-tag, 2 CHPA, 2 sulfate ions, 230 water molecules			Residues 19–226 for chain A, 19–226 for chain B
R_{cryst}/R_{free}	18.4 (41.5)/22.9 (53.6)			23.2 (34.0)/30.7 (44.0)
Average *B*-factor	39.9			70.1
Ramachandran plot: core/allowed/generously allowed	89.5/9.7/0.7			83.6/15.9/0.3
r.m.s.d. bond lengths (Å)	0.024			0.019
r.m.s.d. bond angles (°)	1.989			2.075

[a] DESY, Deutsches Electronen-Synchrotron; SSRL, Stanford Synchrotron Radiation Laboratory.

product of CHPA respiration does not induce transcription of the *cprBA* dehalogenase or significantly interfere with the CHPA-induced allosteric transition.

Allosteric Changes following Binding of ortho-Chlorophenolic Compounds—Although binding of HPA, unlike CHPA, does not elicit a measurable allosteric transition, one can postulate that the local structure of the binding pocket in the HPA-CprK complex is similar to that in the CHPA-CprK complex, given the very high similarity between both compounds. However, as HPA does not induce any DNA binding, the overall structure of the HPA-CprK complex likely resembles that of ligand-free CprK. To model this putative CprK-HPA complex, the β-barrel of the ligand-bound structure was repositioned to occupy the conformation observed in the ligand-free structure. The resulting "hybrid" CprK structure thus contains local active site changes induced by ligand binding, but the overall structure retains the unbound state (Fig. 7*B*). Then, overlaying this hybrid CprK structure on the ligand-free form reveals how ligand binding can induce, among other changes, a large shift in the position of Gly-85 (Fig. 7, *A* and *B*). The repositioning of Gly-85 leads to formation of new hydrogen bonding interactions and direct steric contacts with the chloride atom-binding residues Tyr-130 and Leu-131. This induces reorientation of Tyr-130 and Leu-131 thus reducing the volume of the hydrophobic pocket between the coiled coil helices to exactly match the volume of the chloride atom. The interactions made with CHPA/HPA and the hybrid CprK structure are very similar to those seen in the CHPA-CprK complex except that the phenol hydroxyl group is too distant from Lys-133 to make a direct interaction. In addition, the chloride atom of CHPA is in unfavorably close contacts with Leu-131 and Val-134 as it is positioned slightly off-center from the hydrophobic binding pocket. It seems likely that formation of the phenolate-Lys-133 interaction and the correct positioning of the chloride atom within the hydrophobic pocket drive the rigid body motion of the NH_2-terminal β-barrel (Figs. 3 and 7C).

While the pK_a for the phenol group of HPA is approximately ~10, this value is lowered to ~8.4 in CHPA due to the chloride substituent at the *ortho*-position (Spectrum Laboratories: Chemical Fact Sheet-Chemical Abstract Number 95578). We postulate that CprK can distinguish between CHPA and HPA not only on the basis of the additional steric bulk provided by the chloride atom but also by a "pK_a interrogation" mechanism (35), which is based on the ability of ligands to ionize to the phenolate form and consequently interact with Lys-133, driving the conformational change that promotes DNA binding. Among the several CprK homologues in the genome of *D. hafniense*, Lys-133 is strictly conserved, which supports the pK_a interrogation concept. The other side chain interaction with the phenol hydroxyl group, Tyr-76 is not conserved, and the Y76F variant of *D. hafniense* CprK still undergoes allosteric changes upon binding of CHPA (albeit at 10-fold higher CHPA concentrations than the wild type, Table 2), indicating this residue is not essential for activity. Most residues involved in binding the *ortho*-chlorophenol moiety are conserved or highly similar in CprK paralogs, while residues involved in binding the acetic acid group (*e.g.* Lys/Arg-86, Thr-90, Asn-92) are specific to CprK, indicating that these CprK paralogs will likely interact with other compounds that have been found to serve as terminal electron acceptors such as 2,4-dichlorophenol and/or 2,4,6-trichlorophenol (36).

Downloaded from www.jbc.org at UKB - Universiteitbibliotheek Utrecht on November 16, 2006

CONCLUSIONS

Crystal structures of CprK with and without CHPA bound reveal the binding mode for halogenated orthophenolic compounds and suggest a mechanism whereby both the phenol hydroxyl group and the chloride *ortho*-substituent are required for tight binding and integrally involved in promoting the conformational change that leads to DNA binding. We postulate that binding of CHPA and concomitant phenol deprotonation leads to a rigid body hinge motion of the β-barrel that docks the chloride atom in the binding pocket provided by the central coiled coil and leads to formation of a tight phenolate-Lys-133 interaction. While in absence of a crystal structure for the reduced, CHPA-bound CprK, it is difficult to determine the exact mechanism whereby the observed rigid body motions in the β-barrel are communicated to the DNA-binding domains, we postulate the sensory module reorganization repositions β-strands 3 and 4 with respect to the central coiled coil and allows for a direct contact between the DNA-binding domain and the sensory module to be formed. This disrupts the DNA-binding domain dimer interface and positions the helix-turn-helix motifs in the required conformation for productive binding to the dehalobox DNA. The relative motion of the β-barrel to the B-C helix is reminiscent of similar motions postulated to occur in functionally unrelated proteins containing related sensory modules, such as cyclic nucleotide-gated channels and cAMP- and cGMP-dependent protein kinases (34, 37–40). Formation of a disulfide bond under aerobic conditions between Cys-11 and Cys-200 does not impact CHPA binding but disrupts formation of the correct interdomain contacts and hence provides a possible means for redox regulation of halorespiration.

Acknowledgments—We gratefully acknowledge the use of beamlines at the Deutsches Electronen Synchrotron EBI outstation, Hamburg, Germany. We thank A. J. R. Heck (Utrecht University) for helpful discussions.

REFERENCES

1. Oberg, G. (2002) *Appl. Microbiol. Biotechnol.* **58,** 565–581
2. Henschler, D. (1994) *Angw. Chem. Int. Ed. Engl.* **33,** 1920–1935
3. Gribble, G. W. (2003) *Chemosphere* **52,** 289–297
4. Smidt, H., and de Vos, W. (2004) *Annu. Rev. Microbiol.* **58,** 43–73
5. van de Pas, B. A., Jansen, S., Kijkoma, C., Schraa, G., de Vos, V. M., and Stams, A. J. (2001) *Appl. Environ. Microbiol.* **67,** 3958–3963
6. El Fantroussi, S., Naveau, H., and Agathos, S. N. (1988) *Biotechnol. Prog.* **14,** 167–188
7. Furukawa, K. (2003) *Trends Biotechnol.* **21,** 187–190
8. van de Pas, B. A., Smidt, H., Hagen, W. R., van der Oost, J., Schraa, G., Stams, A. J., and de Vos, V. M. (1999) *J. Biol. Chem.* **274,** 20287–20292
9. Villemur, R., Saucier, M., Gauthier, A., and Beaudet, R. (2002) *J. Microbiol.* **48,** 697–706
10. Smidt, H., van Leest, M., van der Oost, J., and de Vos, V. M. (2000) *J. Bacteriol.* **182,** 5683–5691
11. Pop, S. M., Kolarik, R. J., and Ragsdale, S. W. (2004) *J. Biol. Chem.* **279,** 49910–49918
12. Gabor, K., Verissimo, C. S., Cyran, B. C., Ter Horst, P., Meijer, N. P., Smidt, H., and van der Oost, J. (2006) *J. Bacteriol.* **188,** 2604–2613
13. Korner, H., Sofia, H. J., and Zumft, W. G. (2003) *FEMS Microbiol. Rev.* **27,** 559–592
14. Harman, J. G. (2001) *Biochim. Biophys. Acta* **1547,** 1–17
15. Passner, J. M., Shultz, S. C., and Steitz, T. A. (2000) *J. Mol. Biol.* **304,** 847–859
16. Benoff, B., Yang, H., Lawson, C. L., Parkinson, G., Liu, J., Blatter, E., Ebright, Y. Y., Berman, H. M., and Ebright, R. H. (2002) *Science* **297,** 1562–1566
17. Lawson, C. L., Swigon, D., Murakami, K. S., Darst, S. A., Berman, H. M., and Ebright, R. H. (2004) *Curr. Opin. Struct. Biol.* **14,** 10–20
18. Lanzilotta, W. N., Schuller, D. J., Thorsteinsson, M. V., Kerby, R. L., Roberts, G. P., and Poulos, T. L. (2000) *Nat. Struct. Biol.* **7,** 876–880
19. Eiting, M., Hageluken, G., Schubert, W. D., and Heinz, D. W. (2005) *Mol. Microbiol.* **56,** 433–446
20. Chen, R., and Lee, J. C. (2003) *J. Biol. Chem.* **278,** 13235–13243
21. Yu, S., and Lee, J. C. (2004) *Biochemistry* **43,** 4662–4669
22. Otwinowski, Z., and Minor, W. (1997) *Methods Enzymol.* **276,** 307–326
23. Collaborative Computational Project, Number 4 (1994) *Acta Crystallogr. Sect. D Biol. Crystallogr.* **50,** 760–763
24. Cowtan, K. (1994) *Protein Crystallogr.* **31,** 34–38
25. Roussel, A., and Cambillau, C. (1991) in *Silicon Graphics Geometry Partners Directory 86*, Silicon Graphics, Mountain View, CA
26. Murshudov, G. N., Vagin, A. A., and Dodson, E. J. (1997) *Acta Crystallogr. Sect. D Biol. Crystallogr.* **53,** 240–255
27. Rigaku MSC (1999) *Crysal Clear: Progam Suite for Data Collection and Processing*, Rigaku MSC, Woodlands, TX
28. McCoy, A. J., Grosse-Kunstleve, R. W., Storoni, L. C., and Read, R. J. (2005) *Acta Crystallogr. Sect. D Biol. Crystallogr.* **61,** 458–464
29. Elmsely, P., and Cowtan, K. (2004) *Acta Crytallogr. Sect. D Biol. Crystallogr.* **60,** 2126–2132
30. Winn, M. D., Isupov, M. N., and Murshudob, G. N. (2001) *Acta Crystallogr. Sect. D Biol. Crystallogr.* **57,** 122–133
31. Tahallah, N., Pinkse, M., Maier, C. S., and Heck, A. J. (2001) *Rapid Commun. Mass Spectrom.* **15,** 596–601
32. Krutchinsky, A. N., Chernushevich, I. V., Spicer, V. L., Ens, W., and Standing, K. G. (1998) *J. Am. Soc. Mass Spectrom.* **9,** 569–579
33. Lawrence, M. C., and Colman, P. M. (1993) *J. Mol. Biol.* **234,** 946–950
34. Su, Y., Dostmann, W. R. G., Herberg, F. W., Durick, K., Xuong, N.-H., Ten Eyck, L. F., Taylor, S. S., and Varughese, K. I. (1995) *Science* **269,** 807–813
35. Palfey, B. A., Moran, G. R., Entsch, B., Ballou, D. P., and Massey, V. (1999) *Biochemistry* **38,** 1153–1158
36. Boyer, A., Page-BeLanger, R., Saucier, M., Villemur, R., Lepine, F., Juteau, P., and Beaudet, R. (2003) *Biochem. J.* **373,** 297–308
37. Kaupp, B. U., and Seifert, R. (2002) *Physiol. Rev.* **82,** 769–824
38. Shabb, J. B., and Corbin, J. D. (1992) *J. Biol. Chem.* **267,** 5723–5726
39. Varnum, M. D., Black, K. D., and Zagotta, W. N. (1995) *Neuron* **15,** 619–625
40. Tibbs, G. R., Liu, D. R., Leypold, B. G., and Siegelbaum, S. A. (1998) *J. Biol. Chem.* **273,** 4497–4505

Downloaded from www.jbc.org at UKB - Universiteitsbibliotheek Utrecht on November 16, 2006